

PAPER • OPEN ACCESS

The Structure of Hematite Pigment from Lathe Waste Using Guava Leave Extract by Hydrothermal Method

To cite this article: L M Khoiroh *et al* 2025 *IOP Conf. Ser.: Earth Environ. Sci.* **1439** 012006

View the [article online](#) for updates and enhancements.

You may also like

- [Defect Engineering of Titania and Hematite Thin Films By Advanced Plasma Deposition Triggers High Photoelectrochemical Water Splitting Activity](#)
Štěpán Kment, Alberto Naldoni, Zdenk Hubika et al.
- [Observation and Alterations of Surface States on Hematite Photoelectrodes](#)
Dunwei Wang
- [Thin Hematite Film Based Flavin Microsensor](#)
Gretchen Tibbits, Nathalie A Wall and Haluk Beyenal

UNITED THROUGH SCIENCE & TECHNOLOGY



**248th
ECS Meeting**
Chicago, IL
October 12-16, 2025
Hilton Chicago



**Science +
Technology +
YOU!**

**SUBMIT
ABSTRACTS by
March 28, 2025**

SUBMIT NOW

The Structure of Hematite Pigment from Lathe Waste Using Guava Leave Extract by Hydrothermal Method

L M Khoiroh^{1*}, D A Nisa¹, R F A Akbar¹

¹ Department of Chemistry, UIN Maulana Malik Ibrahim Malang, Malang, Indonesia

* E-mail: lilikmfx@kim.uin-malang.ac.id

Abstract. Lathe waste contains 97% iron, which has the potential as a raw material for producing hematite pigment ($\alpha\text{-Fe}_2\text{O}_3$). Guava leaf extract contains tannin, a reducing agent in synthesizing hematite. In this study, hematite was synthesized using the hydrothermal method at temperatures of 120, 140, and 160°C, then calcined for 3 hours at a temperature of 750°C. XRD, Color reader, FTIR, and SEM characterized the resulting products. The XRD characterization shows that the product before and after calcination was hematite with a rhombohedral structure. Hematite before calcination resulted in an amorphous phase and formed high crystallinity and purity after calcination. The crystal size of hematite ranges from 24.8-34.2 nm. The Color values such as the degree of redness, yellowness, brightness, chroma, and hue are by the hematite pigment standard. The results of FTIR identification on samples before and after calcination have formed hematite with a typical Fe-O group at wave numbers 471 and 575 cm^{-1} . SEM results show that the resulting morphology was not uniform, and aggregate occurs, the necessity for further research to optimize the material's properties, thereby improving its functionality for applications as a pigment and in other relevant fields.

Keywords: Amorphous, Crystalline, Guava Leaf, Hematite, Hydrothermal

1. Introduction

Lathe waste is one of the wastes from iron craft industry that is thrown away to the environmental usually. One way to overcome this pollution is to manage it into materials with economic value, including pigment material. Lathe waste contain 97% of iron that has synthesized to be hematite potentially [1]. According to several research studies, lathe waste can be synthesized to be hematite[2][3]. Khoiroh [4] shows that iron lathe waste may be converted into hematite pigment with dark red color but still there was agglomeration.

Hematite nanoparticles can be synthesized using a hydrothermal technique. This method offers various advantages, including rapid heating, easy reaction, improved outcomes, purity, affordable, save for environmental, and high transformation efficiency [5]. Kongsat [6] explain in their research that hematite was obtained using hydrothermal method were purity hematite with nanoparticle size and spherical morphology. In line with Kongsat, Talibawo [7] was synthesizing hematite using hydrothermal resulting nanoparticle hematite with nanoroad morphology.



The green synthesis of hematite can use natural resources as reductor. In the green synthesise, the using of plant part, such as leaves, branches, roots, and seeds can result the nanoparticle of iron oxide [8] [9] [10]. Plant extracts contain secondary metabolites such as phenolic acid, lignin, flavonoids, and tannins, [11] which can serve as capping agents [12]. The use of plant extracts in synthesis can have an impact on nanoparticle size, shape, and morphology [10]. Guava leaves are one of the plants rich in polyphenols. Active compounds in red guava leaf extract (*Psidium guajava*) include saponins, flavonoids, tannins, eugenol, and triterpenoids, however, flavonoids and tannins are the dominant components. Tannins can operate as precipitating agents because they contain OH groups, which can bind to metals [12], and tannin content in guava leaf extract was $150,05 \pm 4,76$ % [11] has the potential to be a reducing agent. Synthesize hematite use guava leaf extract produced hematite nanoparticles with a diameter 20-50 of nm in irregular shape[13].

The synthesis temperature significantly impacts the crystal structure and crystallinity [5][14]. The degree of crystallinity is controlled by the nucleation process and rapid crystal growth. Iron oxide synthesized using the hydrothermal method at a temperature of 180°C, resulting in hematite (α -FeOOH) structure and β -FeOOH structure at 120°C [5]. At 160°C, resulting in a crystal size of 22 nm, cubic and spherical particle morphologies, and a typical Fe-O group at wave numbers 550 and 434 cm^{-1} . Tadic [14] synthesized hematite at 140°C, achieving a crystal diameter of 20-80 nm and a cubic particle form. In this study, hematite pigment was synthesized from lathe waste using guava leaf extract as a reducing agent which was carried out by the hydrothermal method at various temperatures to test the effect of temperature on structure, color value, functional groups, and shape.

2. Material and Methods

2.1 Material and Instrumentation

The materials used in this investigation are lathe waste, distilled water, HNO_3 p.a (Merck), acetone p.a, NaOH p.a, and guava leaf extract. The instruments used include X-Ray Diffraction (Bruker D8 Advance X-ray diffractometer), Scanning Electron Microscope (Zeiss), Fourier-transform Infrared Spectroscopy (Varian) and a Color reader (Konica Minolta).

2.2. Methods

The precursor solid $\text{Fe}(\text{NO}_3)_3$ 7.5 grams was dissolved in 75 mL of distilled water (ratio 1:10), agitated until homogenous using a magnetic stirrer, and the pH of the solution was determined. After the mixture was uniform, 100 mL of guava leaf extract was gradually added, ensuring it was evenly distributed and swirled with a magnetic stirrer. Next, the pH was measured. The autoclave was heated for 8 hours at 120, 140, and 160°C synthesis temperatures. After the yield and filtrate were formed, the solution was decanted and washed with distilled water to pH 6. Then, it was rinsed with acetone and filtered through a Buchner funnel. Furthermore, the yield was allowed to dry completely at room temperature, resulting in powder. The powder was then calcined in a furnace at 750°C for three hours [4].

3. Result and Discussion

The hydrothermal characterization of the synthesis product before calcination revealed the presence of goethite impurities at $2\theta(o)$: 23 (JCPDS No. 29-0713) with low intensity and large peaks at 120 and 140°C. At a temperature fluctuation of 160°C, the goethite peak diminishes, indicating hematite formation. The demonstrates how the synthesis temperature can influence the degree of crystallinity. The obtained peaks show that the synthesis product has poor crystallinity before calcination, as indicated by the lack of sharp and wide peaks as Figure 1.

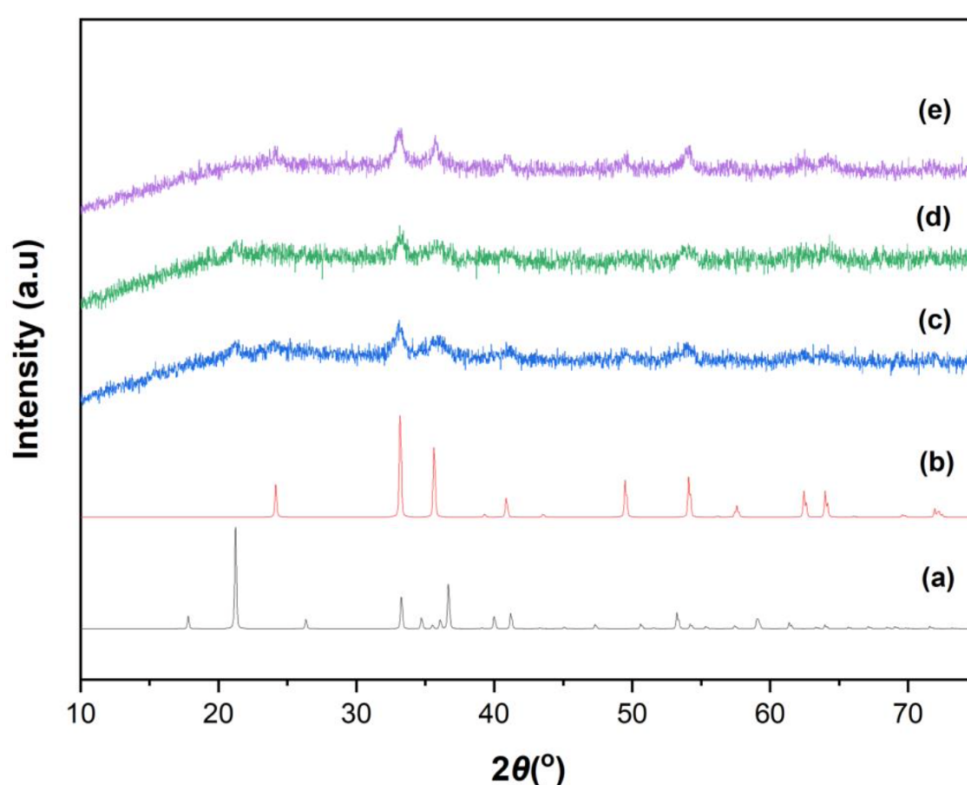


Figure 1. Diffraction Pattern (a) goethite standard (JCPDS No. 29-0713), (b) hematite standard (JCPDS No. 33-0664), (c) hematite at 120°C, (d) hematite at 140°C dan (e) hematite at 160°C

After calcination, the synthesis sample was analyzed by comparing the 2θ peak location to the hematite standard (JCPDS No. 33-0664), as illustrated in Figure 2. The diffraction pattern shows that the synthesis product's three peaks are equal to the standard peak of the hematite compound at the 2θ (o): 33 and 35, with sharp and narrow intensity compared to the synthesis result before calcination. This implies that the heating step influences the crystallinity of the synthesis product. The diffraction pattern's resemblance to the standard demonstrates that the sample is pure hematite, with no additional phases formed. Crystallite size of hematite is ranging from 24.8 to 34.2 nm. These results demonstrate that the synthesis temperature has no major effect on crystallite size.

The hematite sample at 120°C is red. Hematite turns orange-reddish when heated to 140°C. As shown in Figure 3, hematite at 160°C is dark red. Table 1 shows the L^* , C^* , and H^o values of hematite standards and the color analysis results of synthetic hematite samples.

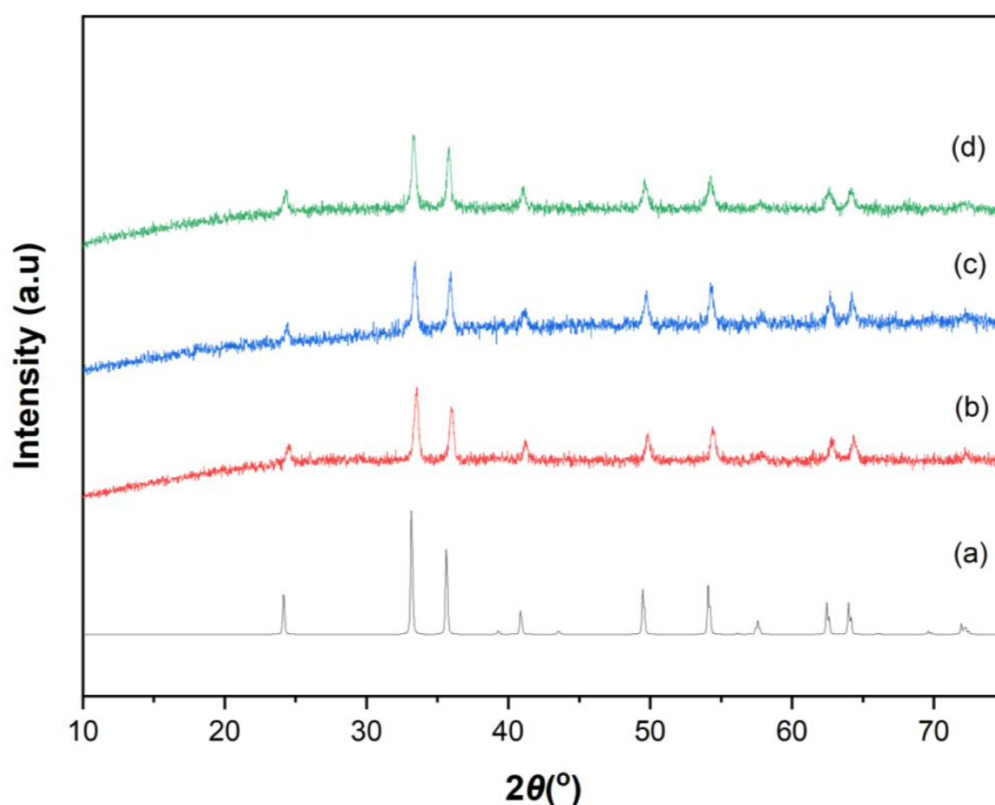


Figure 2. Diffraction pattern of the synthesis results after calcination, (a) hematite standard (JCPDS No. 33-0664), (b) 120, (c) 140, dan (d) 160°C

Table 1. The Color Value of hematite pigment

Temperature (°C)	Color Value				
	L*	C*	H°	a*	b*
Hematite standard	25-45	9-42	21-57		
120°C	40.48	25.92	57.60	13.53	22.11
140°C	37.63	26.94	59.80	12.77	23.71
160°C	41.07	20.20	57.80	9.87	17.6

According to Table 1, the hematite pigment produced during the synthesis falls within the typical range of hematite pigment colors. These findings show that temperature fluctuations have no major effect on the (brightness level) L* value of the synthesis outcomes. At the H° value, the synthesis results surpass the usual hematite range, but not rough, so they remain consistent with the hematite standard. As the synthesis temperature rises, the (green-red degree) a* and (blue-yellow degree) b* values will decrease.

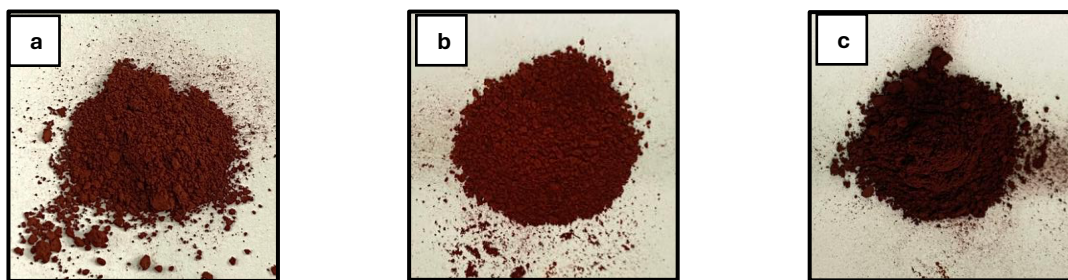


Figure 3. Hematite pigment after calcination (a) 120, (b) 140 dan (c) 160°C

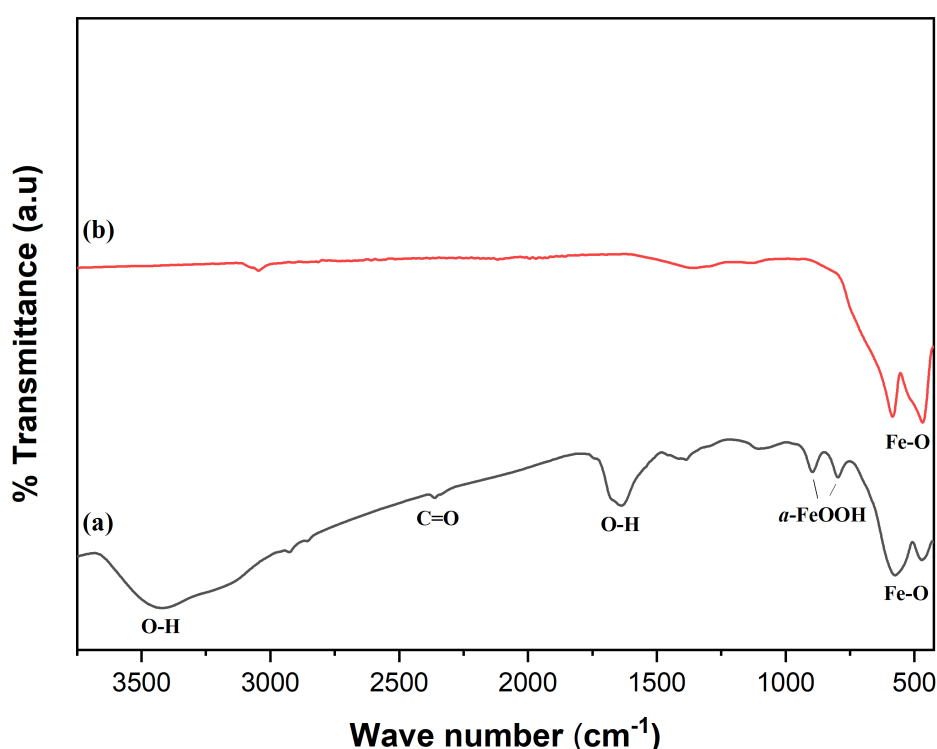


Figure 4. FTIR Spectrum (a) hematite before calcination (b) hematite after calcination

Figure 4 identifies synthesis outcomes at 120°C before and after calcination. At a temperature fluctuation of 120°C before calcination, the absorption of typical hematite compound groups was identified at wave numbers 471 and 575 cm^{-1} , indicating a low-intensity Fe-O stretching vibration mode. Absorption at 797 and 895 cm^{-1} indicates the FeOOH bending vibration in the goethite compound ($\alpha\text{-FeOOH}$) [15]. Absorption at wave number 1637 cm^{-1} suggests the presence of a group of O-H bending caused by water molecules. Absorption at 2361 cm^{-1} suggests that the functional group C=O extends in CO_2 in the atmosphere. The presence of a group at wave number 3418 cm^{-1} denotes the O-H stretching vibrations of polyphenol stretching group [13]. Strong OH group absorption suggests strong OH bonding with the available cations. The synthesis results after calcination revealed that some absorptions were lost, and the intensity increased in the primary molecule compared to before calcination, as shown in Figure 4. The absorption of the usual hematite compound group, Fe-O, showed greater intensity at 471 and 541 cm^{-1} [16]. The normal absorption of secondary metabolites from guava leaves appeared lost due to the high

heating temperature. However, the spectrum in Figure 4 shows that the guava leaf extract has a low concentration. This indicates that the reaction mechanism of hematite formation by guava leaf reductant requires further investigation to identify the true effect.

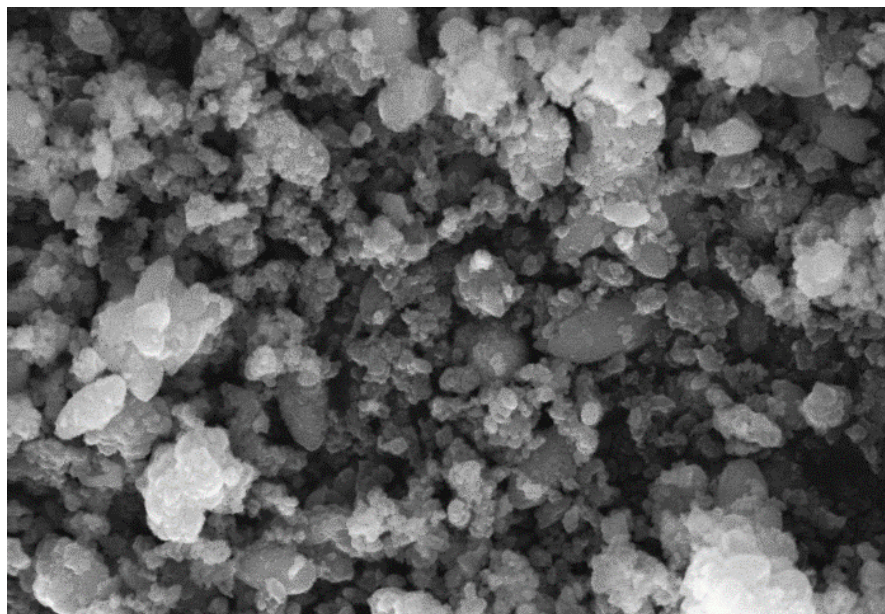


Figure 5. SEM of hematite at 120°C after calcination

SEM characterization of 120°C temperature fluctuations yields round and uneven shapes. Agglomeration is evident at this temperature. The nanometre-sized synthesis products make them easily agglomerated when subjected to excess heat/energy during the calcination process [17]. Furthermore, the synthesis products' XRD diffractograms indicate aggregation due to low crystallinity and noise as Figure 5 depicts the SEM results at a magnification of 25,000x.

4. Conclusion

The synthesis product after precipitation is hematite with goethite impurities, but after calcination, it is hematite with a rhombohedral structure. The size of the generated hematite crystals ranges from 24.8 to 34.2 nm. The color values at various synthesis temperatures align with the hematite pigment standard. Hematite identification using FTIR at 120°C produces typical hematite group absorption, specifically the Fe-O vibration bond at wave numbers 471 and 541 cm^{-1} with acute and strong intensity. The SEM results demonstrate that the morphology is varied, the particle form is mostly spherical, and agglomeration still occurs. Analysis of SEM data indicates the necessity for further research to optimize the material's properties, thereby improving its functionality for applications as a pigment and in other relevant fields.

References

- [1] L. M. Khoiroh, F. Khidin, and R. Ningsih, 2020 *IOP Conf. Ser. Earth Environ. Sci.*, vol. 456, no. 1, p. 012005.
- [2] D. E. Rahmawati, L. M. Khoiroh, R. Ningsih, F. Yusniyanti, W. Solawati, and P. Sari, 2020. *Int. J. Mech. Eng. Technol. Appl.*, vol. 1, no. 2, p. 69.
- [3] L. M. Khoiroh, A. D. A. Sholekah, and E. Yulianti, 2021, *Int. J. Chem.*, vol. 13, no. 1, p. 21.
- [4] L. M. Khoiroh, M. N. Al-Chabib, and A. Prasetyo, 2019, *IOP Conf. Ser. Mater. Sci. Eng.*, vol. 578, no. 1, p. 012004.
- [5] P. A. F. Diniz et al., 2023, *Mater. Res.*, vol. 26, p. e20230016.
- [6] P. Kongsat, K. Kudkaew, J. Tangjai, E. A. O'Rear, and T. Pongprayoon, 2021. *J. Phys. Chem. Solids*, vol. 148, p. 109685.

- [7] J. Talibawo, J. S. Nyarige, P. I. Kyesmen, M. C. Cyulinyana, and M. Diale, *Mater. 2022, Res. Express*, vol. 9, no. 2, p. 026401.
- [8] P. Plachtova, Z. Medříková, R. Zbořil, J. Tuček, R. S. Varma, and B. Maršálek, 2018, *ACS Sustainable Chem. Eng.* 6:8679–8687.
- [9] J. Jeyasundari, P. S. Praba, Y. B. A. Jacob, V. S. Vasantha, and V. Shanmugaiah, 2017, *Chem Sci Rev Lett*, 6(22), 1244–1252.
- [10] G. Ksv, J. 2017, *Nanomedicine Biotherapeutic Discov.*, vol. 07, no. 01.
- [11] S. D. Sornapudi and M. Srivastava, “Quantitative estimation of phytochemicals in different leaf extracts”.
- [12] S. P. Patil and P. M. Rane, 2020, *Beni-Suef Univ. J. Basic Appl. Sci.*, vol. 9, no. 1, p. 60.
- [13] A. Rufus, N. Sreeju, and D. Philip, 2019, *J. Phys. Chem. Solids*, vol. 124, pp. 221–234
- [14] B. Ahmmad et al., *Adv. Powder Technol.*, vol. 24, no. 1, pp. 160–167, Jan. 2013.
- [15] N. Madubuonu et al., 2020, *Appl. Phys. A*, vol. 126, no. 1, p. 72.
- [16] P. R. S. Baabu, H. K. Kumar, M. B. Gumpu, J. Babu K, A. J. Kulandaisamy, and J. B. B. Rayappan, 2022, *Materials*, vol. 16, no. 1, p. 59.
- [17] M. Su, C. He, and K. Shih, 2016, *Ceram. Int.*, vol. 42, no. 13, pp. 14793–14804